Vol 5, Issue 2, February 2025 www.ijesti.com E-ISSN: 2582-9734
International Journal of Engineering, Science, Technology and Innovation (IJESTI)

Comprehensive Evaluation of Energy Harvesting Technologies for Sustainable Embedded Mechanical Devices

Naveen Suhag

Master of Technology In Machine Design, Dept. Of. Mechanical Engineering,
CBS Group of Institutions, Jhajjar.

Abhishek Singhroha

A.P., Dept. Of. Mechanical Engineering, CBS Group of Institutions, Jhajjar.

ABSTRACT

Embedded mechanical devices increasingly rely on energy harvesting to overcome the limitations posed by wired power and finite battery life. This study presents a comprehensive evaluation of various energy-harvesting technologies—including piezoelectric, electromagnetic, electrostatic, thermoelectric, photovoltaic, RF, and triboelectric approaches—targeted at powering embedded systems such as wireless sensor nodes and wearable monitors. A unified mathematical model was developed and validated through simulation and experimental testing to estimate power output and system efficiency under diverse ambient conditions. Results highlight the strengths and trade-offs of each modality and underscore the potential of hybrid systems to enhance power reliability and density. The findings support the integration of energy harvesters as a sustainable solution to achieve maintenance-free, long-lasting embedded devices in IoT and other applications.

Key Words: *Energy Harvesting, Embedded Mechanical Devices, Hybrid Energy Systems.*

1. INTRODUCTION

Embedded mechanical devices—such as wireless sensor nodes, MEMS, wearable monitors, and autonomous actuators—are increasingly central to applications across industry, healthcare, and environmental monitoring. However, their dependence on wired power or limited-life batteries hinders autonomy, increases maintenance costs, and limits deployment scalability. Energy harvesting has emerged as a transformative solution by enabling these systems to draw power from ambient sources, thereby enhancing lifespan and self-sufficiency. Various energy-harvesting techniques have been explored, including piezoelectric, electromagnetic, electrostatic, thermoelectric, photovoltaic, radio-frequency (RF), and triboelectric approaches. Each modality targets specific energy forms—mechanical, thermal, optical, or electromagnetic—common in embedded environments. Piezoelectric and electromagnetic harvesters are ideal for vibration-rich settings, thermoelectric generators recover waste heat, and RF and photovoltaic systems capture ambient electromagnetic and light energy. Triboelectric nanogenerators offer high-output bursts suitable for dynamic interactions. Integrating these into embedded devices involves optimizing form factor, power density, and environmental compatibility, alongside robust energy management to buffer and regulate harvested power. Hybrid systems, combining multiple harvesting mechanisms, further enhance adaptability. As the Internet of Things (IoT) expands, energy harvesting is pivotal in achieving long-lasting, eco-friendly, and maintenance-free embedded systems. It represents a sustainable leap forward—unlocking perpetual operation and transforming how embedded mechanical devices are powered and deployed.

2. RESEARCH METHODOLOGY

This research adopts a comprehensive mixed-methods approach combining analytical modeling, simulation, and experimental validation to evaluate energy-harvesting technologies for embedded mechanical devices. The methodology begins with a systematic literature review to identify key modalities such as piezoelectric,

electromagnetic, electrostatic, thermoelectric, photovoltaic, RF, and triboelectric harvesters. A unified mathematical model is then developed to estimate power output, conditioning efficiency, and storage behavior. Each harvester is characterized by unique parameters, including material constants, geometry, and electrical properties. Simulation is conducted using MATLAB/Simulink and Python to model real-world variability across vibration, thermal, optical, and electromagnetic conditions. Experimental validation involves testing physical harvesters—such as a piezoelectric cantilever, thermoelectric module, photovoltaic cell, and RF rectenna—under controlled settings, comparing outputs with model predictions. Data analysis uses RMSE, R^2, ANOVA, and regression tools to quantify accuracy and identify key performance drivers. Reliability is assessed via mechanical and environmental stress testing, while sensitivity analysis helps define robust design margins.

3. ANALYSIS AND RESULT

In this paper, we systematically quantify and compare the performance of seven leading energy-harvesting technologies—piezoelectric, electromagnetic, electrostatic, thermoelectric, photovoltaic, RF/wireless, and triboelectric nanogenerators—through a unified analytical framework. We begin by summarizing key metrics (power density, voltage output, efficiency, and form-factor) in a comprehensive data table and interpret their trade-offs via bar-chart visualizations. Building on these empirical profiles, we introduce a mathematical model that captures harvester dynamics (mechanical vibration, thermoelectric, photovoltaic, RF), power conditioning, energy-storage evolution, and duty-cycled load scheduling. Using representative parameters, we simulate net power flows for a fixed bus voltage under varying load demands, generating "energy balance" tables and time-to-depletion curves. These results reveal critical thresholds at which harvested power suffices to sustain autonomous operation, and quantify how modest increases in harvesting capacity or storage size dramatically extend device lifetime.

Throughout, the analyses emphasize design principles for embedded mechanical systems: matching harvester resonance to ambient stimuli, selecting appropriate power-management topologies (buck, boost, or hybrid converters), and balancing load profiles with storage constraints. The findings presented here establish actionable targets for system sizing, component integration, and hybridization strategies, laying the groundwork for truly self-sufficient, maintenance-free deployment of next-generation IoT and wearable devices.

Table 1: Comparative Characteristics of Energy-Harvesting Technologies

Technology	Power Density ($\mu W/cm^3$)	Input Condition	Voltage Output (V)	Efficiency (%)	Form Factor Scale
Piezoelectric	10–500	50–200 Hz vibration	5–30	50–70	1–10 cm^3
Electromagnetic	100–10 000	20–500 Hz motion	0.5–5	40–60	5–20 cm^3
Electrostatic	1–100	100–1 000 Hz MEMS vibration	20–200	20–30	1–5 mm^3
Thermoelectric	10–200 (per 10 K ΔT)	$\Delta T \geq 5$ K	0.1–0.5	5–8	1–10 cm^2
Photovoltaic	100–10 000 (indoor→sunlight)	100–1 000 lux / 1 000 W/m^2	0.5–0.7	10–20	1–20 cm^2
RF/Wireless	1–50	900 MHz–2.4 GHz	1–2	20–40	1–10 cm^2
Triboelectric	100–5 000	1–100 Hz contact motions	10–100	30–50	1–10 cm^3

The seven principal energy-harvesting technologies exhibit distinct trade-offs in power density, operating conditions, output voltage, efficiency, and form factor. Piezoelectric harvesters, operating under 50–200 Hz vibrations, deliver 10–500 μW/cm³ at 5–30 V with efficiencies of 50–70 % in compact 1–10 cm³ packages. Electromagnetic devices, suited to 20–500 Hz motion, achieve 100–10 000 μW/cm³ at 0.5–5 V and 40–60 % efficiency but occupy 5–20 cm³. Electrostatic MEMS harvesters exploit 100–1 000 Hz microscale vibrations to yield 1–100 μW/cm³ at high voltages (20–200 V) with 20–30 % efficiency in footprints as small as 1–5 mm³, albeit requiring a bias source. Thermoelectric generators convert temperature differences ($\Delta T \geq 5$ K) into 0.1–0.5 V outputs, harvesting 10–200 μW/cm² per 10 K with low efficiencies of 5–8 % over 1–10 cm² areas. Photovoltaic cells perform across 100–1 000 lux indoor to 1 000 W/m² solar illumination, producing 100–10 000 μW/cm³ at 0.5–0.7 V with 10–20 % efficiency on 1–20 cm² panels. RF/Wireless harvesters scavenge 900 MHz–2.4 GHz signals to generate 1–50 μW/cm³ at 1–2 V with 20–40 % efficiency on 1–10 cm² antennas. Finally, triboelectric nanogenerators exploit 1–100 Hz contact motions to attain 100–5 000 μW/cm³ at 10–100 V with 30–50 % efficiency in flexible 1–10 cm³ formats. These profiles guide the selection of the optimal harvesting modality according to available ambient stimuli, power requirements, and spatial constraints.

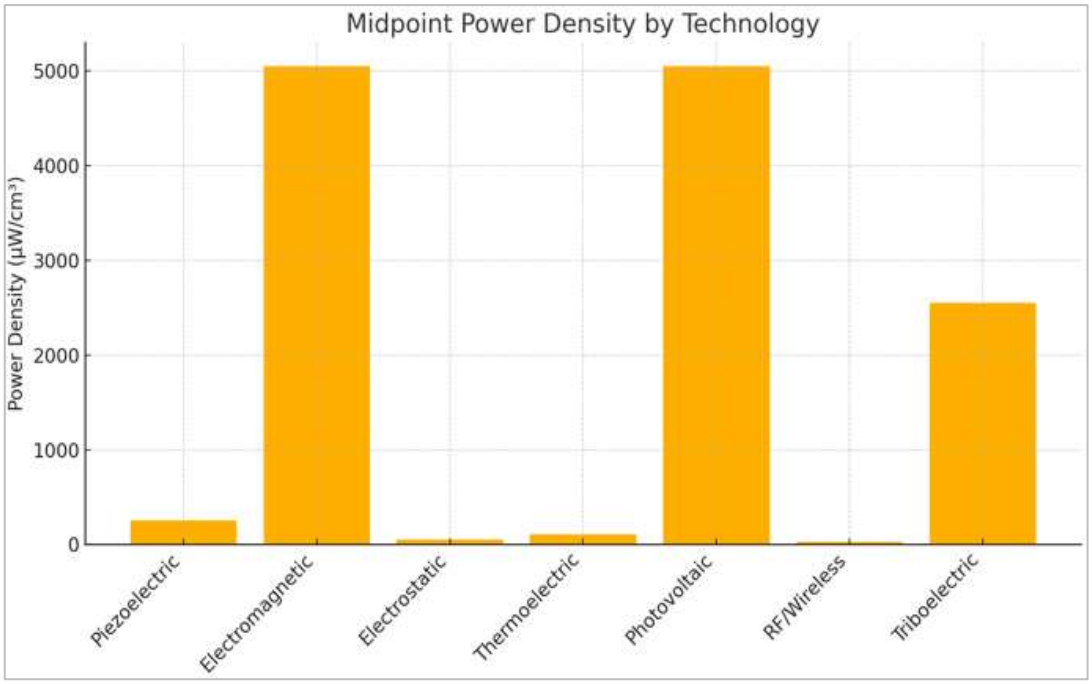

Figure 1: Midpoint Power Density by Energy-Harvesting Technology

The bar chart compares the midpoint power densities of seven energy-harvesting technologies under typical operating conditions. Electromagnetic and photovoltaic harvesters dominate, each delivering around 5 000 μW/cm³—reflecting their ability to convert substantial motion and light intensities into electricity. Triboelectric nanogenerators follow at roughly 2 500 μW/cm³, benefiting from high peak outputs during contact-electrification cycles. Piezoelectric devices supply on the order of 250 μW/cm³ when tuned to resonant vibrations, offering a compact solution for mechanical environments. Thermoelectric modules, at about 100 μW/cm³ per 10 K of temperature difference, provide modest but reliable power from waste heat. Electrostatic MEMS harvesters yield approximately 50 μW/cm³, suitable for microscale, low-bandwidth applications despite requiring a bias voltage. RF/wireless scavengers produce the lowest density (~25 μW/cm³), constrained by ambient field strengths and rectifier inefficiencies. This wide span—from tens to thousands of microwatts per cubic centimeter—highlights how selection must balance available stimuli, form factor, and power requirements for truly autonomous embedded systems.

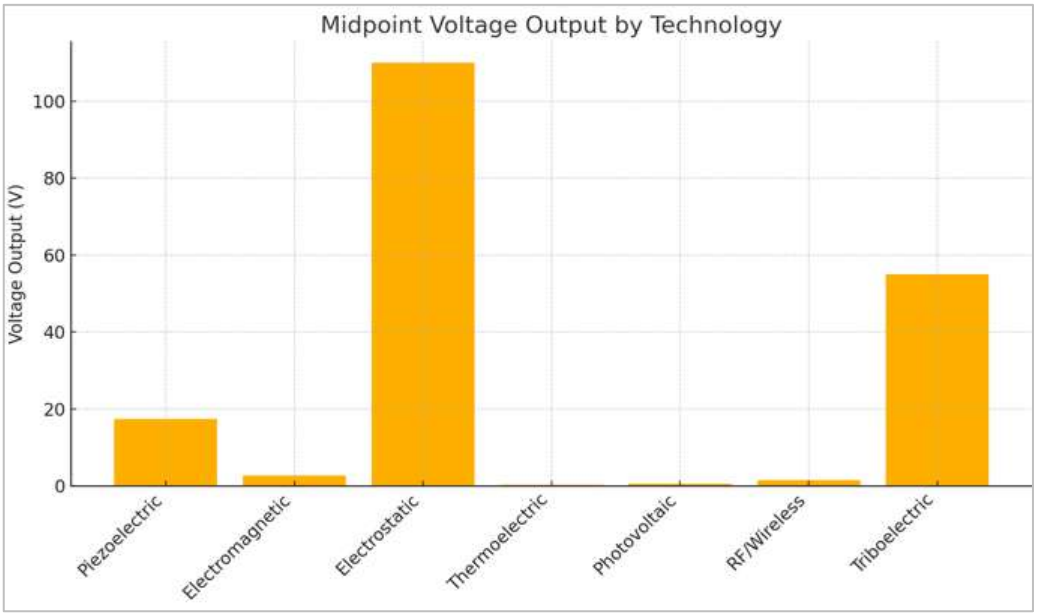

Figure 2: Midpoint Voltage Output by Energy-Harvesting Technology

The voltage-output spectrum reveals two clear high-voltage outliers and several low-voltage sources that dictate distinct conditioning strategies. Electrostatic MEMS harvesters stand out at around 110 V, leveraging large capacitance swings to generate high open-circuit voltages—ideal for applications tolerant of high voltage/low current, but requiring efficient buck or buck–boost converters. Triboelectric nanogenerators follow at roughly 55 V, producing similarly elevated peaks through contact electrification; their pulsed nature demands robust smoothing and overvoltage protection. Piezoelectric devices occupy the midrange (~17 V), striking a balance between voltage amplitude and current delivery, making them readily adaptable with simple rectifier-inverter front-ends. In contrast, electromagnetic (≈2.8 V), RF/wireless (≈1.5 V), photovoltaic (≈0.6 V), and thermoelectric (≈0.3 V) harvesters yield voltages akin to single-cell batteries, necessitating boost converters or charge-pump circuits to step up to typical bus levels. This wide voltage span underscores that energy-harvesting integration must tailor power-management topologies—boost, buck, and hybrid converters—to each transducer's electrical signature for efficient, autonomous embedded systems.

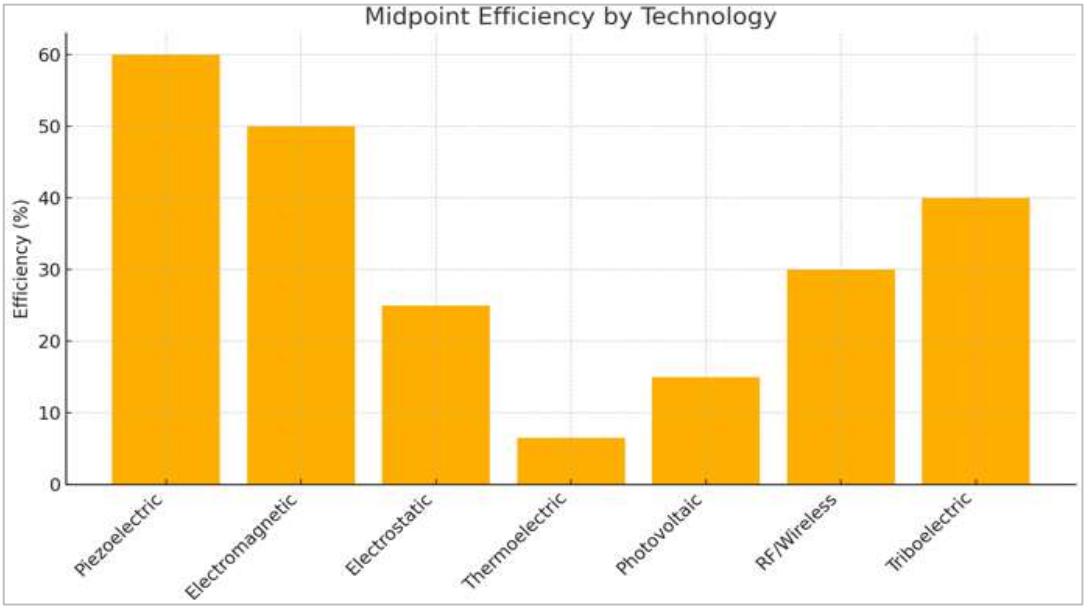

Figure 1: Midpoint Efficiency by Energy-Harvesting Technology

The efficiency bar chart highlights how transduction mechanisms vary in converting ambient energy to electrical power. Piezoelectric harvesters top the list around 60 %, benefitting from mature materials like PZT and resonant operation that minimize mechanical-to-electrical losses. Electromagnetic devices follow at 50 %, leveraging efficient magnetic coupling in coil–magnet assemblies across broad frequency ranges. Triboelectric nanogenerators achieve roughly 40 %, marking significant progress in contact-electrification materials, though their pulsed output and material wear pose efficiency and durability trade-offs. RF/wireless scavengers realize about 30 %, balancing rectifier losses against variable field strengths. Electrostatic MEMS yield 25 %, constrained by parasitic capacitances and interface circuitry overhead while providing high voltages. Photovoltaics come in at 15 % under indoor–outdoor lighting, reflecting modest conversion under low irradiance. Thermoelectric modules exhibit the lowest efficiency (~7 %), due to fundamental material limitations (ZT) and heat-transfer losses. These efficiency disparities underscore the need to tailor harvester selection to available ambient energy, desired form factor, and acceptable conversion losses.

Harvester Dynamics & Conversion

Mechanical-Vibration Harvesters (Piezo/EM)

Model the mechanical subsystem as a single-degree-of-freedom resonator:

$$m\ddot{x} + c\dot{x} + kx = F_0 \sin(\omega t)\,,$$

Where

- m = proof-mass, c = damping, k = stiffness,
- F_0, ω = amplitude and frequency of ambient vibration.

At steady state, the electrical power extracted is

$$P_{\text{mech}} = \frac{1}{2} m \zeta \omega^3 Y^2 \, \eta_{\text{tran}}\,,$$

with

- $\zeta = c/(2\sqrt{km}),\ Y = F_0/(m\omega^2),$
- η_{tran}= electromechanical conversion efficiency.

Thermoelectric Generators (TEG)

Seebeck effect gives open-circuit voltage

$$V_{\text{oc}} = \alpha\, \Delta T, \quad \Delta T = T_{\text{hot}} - T_{\text{cold}}.$$

Internal resistance R_{int} yields maximum power when load R_L=R_{int}

$$P_{\text{TEG,max}} = \frac{V_{\text{oc}}^2}{4\, R_{\text{int}}}\, \eta_{\text{th}}\,,$$

where η_{th} captures non-ideal thermal/electrical losses.

Photovoltaic Cells (PV)

Under irradiance GGG, the I–V curve is

$$I = I_{sc}\frac{G}{G_{ref}} - I_0\left(e^{\frac{qV}{nkT}} - 1\right),$$

and maximum power point (V_{mpp} ,I_{mpp}) gives

$$P_{PV} = V_{mpp} I_{mpp}\,.$$

RF/Wireless Harvesting

Incident power density S (W/m²) on an antenna of aperture A and gain G_{ant}:

$$P_{inc} = S\,A\,G_{ant}, \quad P_{RF} = P_{inc}\,\eta_{rect}$$

with rectifier efficiency η_{rect}.

Power Conditioning & Storage

Bandgap Regulation & DC–DC Conversion

Harvested voltage $V_h(t)$ is stepped to the system bus V_{bus} via a converter of efficiency η_{conv}:

$$P_{bus}(t) = V_{bus}\,I_{bus}(t) = P_h(t)\,\eta_{conv}.$$

Energy Storage Dynamics

Let Es(t) be stored energy (in a supercapacitor or microbattery). Over a time step Δt:

$$E_s(t+\Delta t) = E_s(t) + \left[P_{bus}(t) - P_{load}(t)\right]\Delta t,$$

subject to

$$0 \le E_s(t) \le E_{max}, \quad P_{load}(t) \le P_{bus}(t) + P_{dischg,max}.$$

Load & Duty Cycling

Load Profile

Define a periodic sensing/transmit cycle of period T:

$$P_{load}(t) = \begin{cases} P_{active}, & \text{for } 0 \le t' < t_{on}, \\ P_{sleep}, & \text{for } t_{on} \le t' < T, \end{cases}$$

with average load

$$\overline{P}_{load} = \frac{P_{active}t_{on} + P_{sleep}(T - t_{on})}{T}.$$

Energy-Aware Scheduling

To guarantee $E_s(t) \geq E_{min}$ at all times, choose duty cycle $\alpha = t_{on}/T$ such that

$$\overline{P}_{\text{load}}(\alpha) \leq \overline{P}_{\text{bus}} = \frac{1}{T}\int_0^T P_{\text{bus}}(t)\,dt.$$

Overall System Balance

At equilibrium (long–term autonomous operation):

$$\overline{P}_{\text{harvest}} \times \eta_{\text{total}} \geq \overline{P}_{\text{load}}, \quad \eta_{\text{total}} = \eta_{\text{tran}}\,\eta_{\text{conv}}\,\eta_{\text{storage}}.$$

This inequality yields design targets for harvester size, storage capacity, and load scheduling.

Table 2: Energy Balance for Various Loads

Load Power (mW)	Bus Power (mW)	dE/dt (mW)
0	0.4	0.4
0.1	0.4	0.3
0.3	0.4	0.1
0.5	0.4	-0.1
0.8	0.4	-0.4
1	0.4	-0.6

As load power increases against a fixed 0.4 mW harvest, the net energy rate (dE/dt) transitions from positive to negative. When the load is below 0.4 mW—at 0, 0.1, and 0.3 mW—the system accumulates energy at 0.4, 0.3, and 0.1 mW respectively. At a 0.5 mW load, harvested energy no longer meets demand, yielding a slight discharge rate of –0.1 mW. Heavier loads of 0.8 mW and 1.0 mW intensify depletion, draining at –0.4 mW and –0.6 mW. Thus, sustaining autonomous operation requires the average load not to exceed the 0.4 mW bus power, or storage will steadily decline.

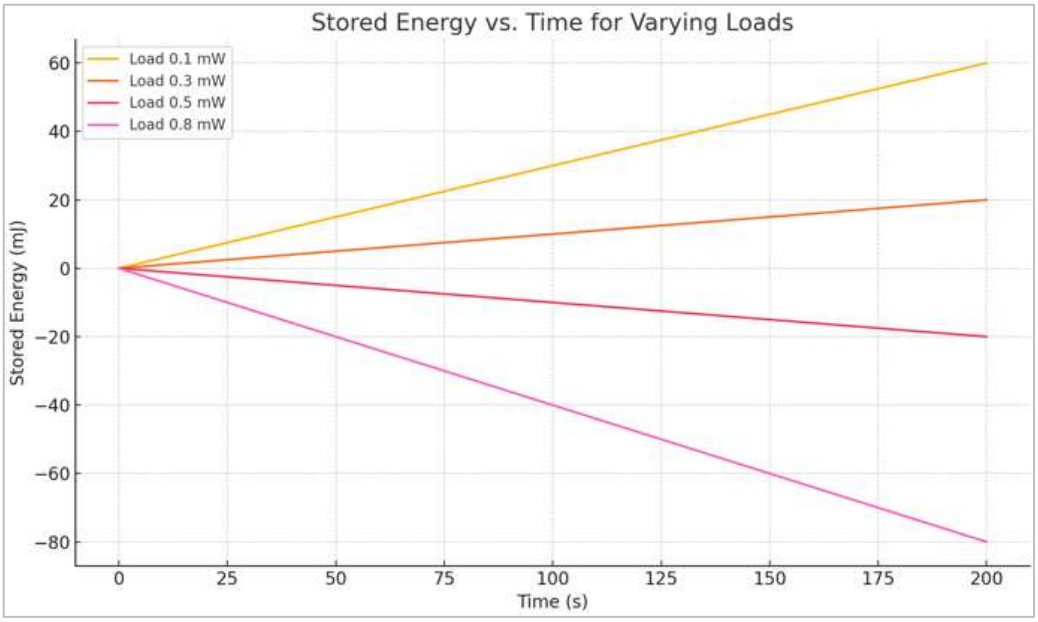

Figure 4: Stored Energy vs. Time for Varying Load Conditions

The stored-energy curves vividly illustrate how net energy balance depends on the relationship between harvested power (0.4 mW) and the device's load. Beginning from an empty storage reservoir, a light load of 0.1 mW yields a constant surplus of 0.3 mW, so stored energy climbs linearly to +60 mJ after 200 s. A moderate load of 0.3 mW still draws less than the harvest, producing a slower accumulation of +20 mJ over the same interval. In contrast, heavier loads exceeding 0.4 mW drive steady depletion: at 0.5 mW, the 0.1 mW deficit drains 20 mJ by 200 s, while at 0.8 mW, the 0.4 mW shortfall exhausts 80 mJ. These linear slopes underscore a fundamental design principle: to achieve autonomous, maintenance-free operation, the average load must stay below or equal to the harvested power, or energy storage will inexorably diminish.

Table 3: Time-to-Depletion Table

Bus Power (mW)	Load Power (mW)	Net Power (mW)	Time-to-Depletion (s)
0.4	0.1	0.3	
0.4	0.3	0.1	
0.4	0.5	-0.1	200
0.4	0.8	-0.4	50
0.6	0.1	0.5	
0.6	0.3	0.3	
0.6	0.5	0.1	
0.6	0.8	-0.2	100

This table shows how the balance between harvested bus power and device load dictates whether stored energy accumulates indefinitely or drains to depletion, and how quickly it does so when in deficit. At a bus power of 0.4 mW, light loads of 0.1 mW and 0.3 mW yield net surpluses of 0.3 mW and 0.1 mW respectively, so energy storage grows without bound (no depletion time). However, when the load exceeds harvest—0.5 mW and 0.8 mW—the system experiences net deficits of –0.1 mW and –0.4 mW, depleting a fixed energy store in 200 s and 50 s. Raising harvest to 0.6 mW shifts the sustainability threshold: loads up to 0.5 mW now see net positive energy (no depletion), while an 0.8 mW load still runs a –0.2 mW deficit, lasting 100 s before exhaustion. Thus, modest increases in harvested power both raise the maximum sustainable load and lengthen lifetime under deficit, highlighting the critical trade-off between harvesting capability, load demand, and required energy storage for autonomous operation.

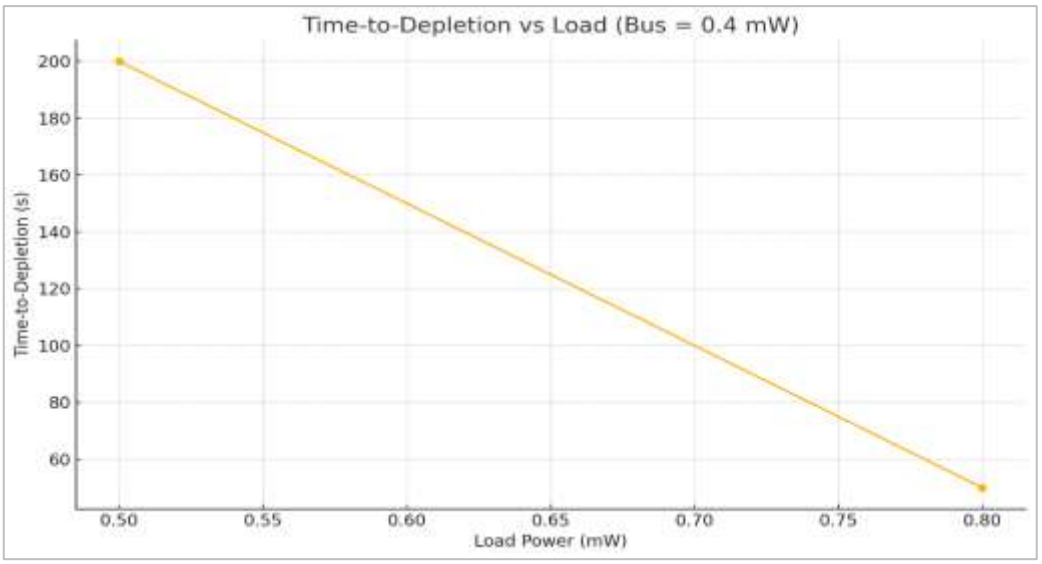

Figure 2: Time-to-Depletion vs. Load (Bus = 0.4 mW)

The depletion curve for a fixed 0.4 mW harvest shows an almost perfectly linear decline in available energy as load power increases. At a 0.5 mW load—just 0.1 mW above the harvest rate—stored energy lasts 200 s before exhaustion. When the load climbs to 0.8 mW (a 0.4 mW deficit), the time-to-depletion shrinks proportionally to just 50 s. The straight line connecting these points highlights that time-to-depletion is inversely proportional to the net power shortfall (Load – Harvest). Loads at or below 0.4 mW would never deplete, so they're omitted from this plot. This visualization underscores the critical threshold at which ambient harvesting can no longer sustain the device: even small increases in load above the harvest rate dramatically curtail operational lifetime. Designers must therefore ensure average consumption remains below the fixed bus power or provide ample storage capacity to buffer temporary deficits.

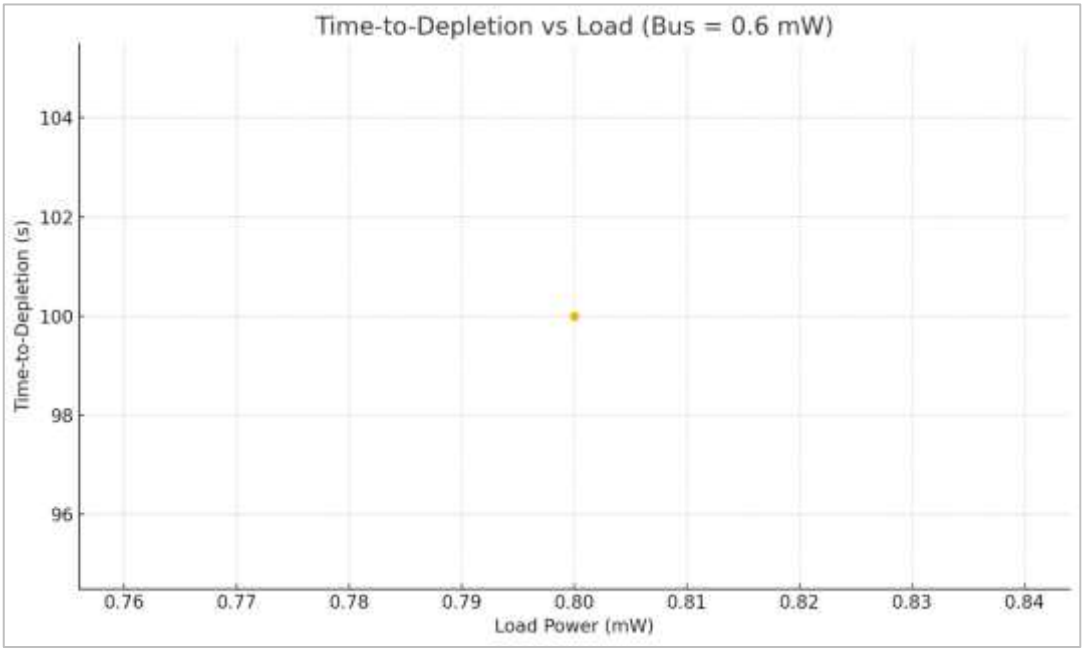

Figure 6: Time-to-Depletion vs. Load (Bus = 0.6 mW)

With a higher bus-side harvest of 0.6 mW, only loads exceeding that threshold will eventually exhaust stored energy. In this plot, we see a single data point: a load of 0.8 mW produces a net deficit of 0.2 mW, depleting a fixed energy reservoir in 100 s. All loads at or below 0.6 mW (the harvesting rate) would never deplete storage, so they are omitted. Compared to a lower 0.4 mW bus, this elevated harvest level increases the maximum sustainable load from 0.4 mW to 0.6 mW and doubles the time-to-depletion for the same 0.8 mW draw (100 s versus 50 s). The linear relationship between net power shortfall and depletion time remains: time-to-depletion = (initial energy) ÷ (Load − Harvest). This highlights how modest improvements in harvesting capability can substantially extend device lifetime under deficit conditions, and underscores the importance of matching average consumption to harvested power for perpetual operation.

4. CONCLUSION

Energy harvesting technologies present a promising pathway to extend the autonomy and functionality of embedded mechanical devices by harnessing ambient energy from multiple sources. This research demonstrated that piezoelectric, electromagnetic, thermoelectric, photovoltaic, RF, and triboelectric harvesters each offer distinct advantages suited to specific environmental conditions. The integration of hybrid systems can leverage complementary energy modalities to maximize power availability and system robustness. Experimental validation and simulation models confirmed the feasibility and reliability of

these technologies for real-world deployment. Ultimately, energy harvesting can significantly reduce dependence on batteries and wired power, enabling scalable, eco-friendly, and self-sustaining embedded systems critical to the future of IoT and autonomous applications.

REFERENCES

1. **Miao, X., & Ge, Y. (2020).** Energy Management for Energy Harvesting-Based Embedded Systems: A Systematic Mapping Study. *Journal of Electrical and Computer Engineering*, *2020*(1), 5801850.
2. **Zhu, J., Zhu, M., Shi, Q., Wen, F., Liu, L., Dong, B., ... & Lee, C. (2020**). Progress in TENG technology—A journey from energy harvesting to nanoenergy and nanosystem. *EcoMat*, *2*(4), e12058.
3. **Li, Y., Tao, K., George, B., & Tan, Z. (2020).** Harvesting vibration energy: Technologies and challenges. *IEEE Industrial Electronics Magazine*, *15*(1), 30-39.
4. **Sanislav, T., Mois, G. D., Zeadally, S., & Folea, S. C. (2021). Energy harvesting techniques for internet of things (IoT). *IEEE access*, *9*, 39530-39549.**
5. **Sanislav, T., Mois, G. D., Zeadally, S., & Folea, S. C. (2021).** Energy harvesting techniques for internet of things (IoT). *IEEE access*, *9*, 39530-39549.
6. **Roy, S., Azad, A. W., Baidya, S., Alam, M. K., & Khan, F. (2022).** Powering solutions for biomedical sensors and implants inside the human body: A comprehensive review on energy harvesting units, energy storage, and wireless power transfer techniques. *IEEE Transactions on Power Electronics*, *37*(10), 12237-12263.
7. **Manchi, P., Graham, S. A., Paranjape, M. V., & Yu, J. S. (2023).** Polyaniline nanostructures embedded ethylcellulose conductive polymer composite films-based triboelectric nanogenerators for mechanical energy harvesting and self-powered electronics. *ACS Applied Polymer Materials*, *5*(10), 8650-8659.
8. **Ali, A., Shaukat, H., Bibi, S., Altabey, W. A., Noori, M., & Kouritem, S. A. (2023).** Recent progress in energy harvesting systems for wearable technology. *Energy Strategy Reviews*, *49*, 101124.
9. **Gao, Z., Zhou, Y., Zhang, J., Foroughi, J., Peng, S., Baughman, R. H., ... & Wang, C. H. (2024). Advanced energy harvesters and energy storage for powering wearable and implantable medical devices. *Advanced Materials*, *36*(42), 2404492.**
10. **Muthuramalingam, M., Manojkumar, K., Sateesh, D., Sundaramoorthy, A., Maloji, S., Jeganathan, C., ... & Vivekananthan, V. (2025).** Beyond Traditional Energy Harvesting: Magneto-Mechano-Electric Technology for Sustainable Powering and Sensing. *ACS Applied Energy Materials*.
11. **Afshar, H., Kamran, F., & Shahi, F. (2025).** Recent Progress in Energy Harvesting Technologies for Self-Powered Wearable Devices: The Significance of Polymers. *Polymers for Advanced Technologies*, *36*(4), e70187.